



Research article

Evaluation of the synergistic potential and mechanisms of action for *de novo* designed cationic antimicrobial peptides

Margarita Karapetian^a, Evgenia Alimbarashvili^{a,b}, Boris Vishnepolsky^b,
 Andrei Gabrielian^c, Alex Rosenthal^c, Darrell E. Hurt^c, Michael Tartakovsky^c,
 Mariam Mchedlishvili^a, Davit Arsenadze^a, Malak Pirtskhalava^b,
 Giorgi Zaalishvili^{a,b,*}

^a Laboratory of Chromatin Biology, Institute of Cellular and Molecular Biology, Agricultural University of Georgia, 240 David Aghmashenebeli Alley, 0159, Tbilisi, Georgia

^b Ivane Beritashvili Center of Experimental Biomedicine, 0160, Tbilisi, Georgia

^c Office of Cyber Infrastructure and Computational Biology, National Institute of Allergy and Infectious Diseases, National Institutes of Health, Bethesda, MD, 20892, USA

ARTICLE INFO

Keywords:

CAMP
 AMP
 Synergy
 E. coli

ABSTRACT

Antimicrobial peptides (AMPs) have emerged as promising candidates in combating antimicrobial resistance – a growing issue in healthcare. However, to develop AMPs into effective therapeutics, a thorough analysis and extensive investigations are essential. In this study, we employed an *in silico* approach to design cationic AMPs *de novo*, followed by their experimental testing. The antibacterial potential of *de novo* designed cationic AMPs, along with their synergistic properties in combination with conventional antibiotics was examined. Furthermore, the effects of bacterial inoculum density and metabolic state on the antibacterial activity of AMPs were evaluated. Finally, the impact of several potent AMPs on *E. coli* cell envelope and genomic DNA integrity was determined. Collectively, this comprehensive analysis provides insights into the unique characteristics of cationic AMPs.

1. Introduction

Standard antibiotics are becoming less effective for clinical use due to the emergence and spread of antimicrobial resistance. The Centers for Disease Control and Prevention (CDC) and the World Health Organization (WHO) have recognized antibiotic resistance as a “global public health concern” [1]. Among the pathogens posing the greatest threat to human health are Gram-negative bacteria resistant to multiple antibiotics. For deaths attributable to antimicrobial resistance *E. coli* was responsible for most deaths in 2019 [2]. Hence, there is an urgent need for the discovery and development of novel drugs that can effectively treat bacterial infections induced by particularly drug-resistant Gram-negative bacteria [3]. Antimicrobial peptides (AMPs) have the potential to become new therapeutic agents in the fight against bacterial resistance [1,4,5]. Unlike traditional antibiotics, which target specific biomolecules in bacterial cells, AMPs have been shown to exhibit multiple modes of action with non-specific targets and are less prone to induce

* Corresponding author Laboratory of Chromatin Biology, Institute of Cellular and Molecular Biology, Agricultural University of Georgia, 240 David Aghmashenebeli Alley, 0159, Tbilisi, Georgia.

E-mail address: gi.zaalishvili@agruni.edu.ge (G. Zaalishvili).

<https://doi.org/10.1016/j.heliyon.2024.e27852>

Received 23 June 2023; Received in revised form 1 March 2024; Accepted 7 March 2024

Available online 13 March 2024

2405-8440/© 2024 The Authors. Published by Elsevier Ltd. This is an open access article under the CC BY-NC-ND license (<http://creativecommons.org/licenses/by-nc-nd/4.0/>).

resistance [6,7].

The antimicrobial activity of most AMPs is strongly related to their physicochemical properties, such as charge, hydrophobicity, isoelectric point, etc. [8,9]. It has been widely acknowledged that high cationic charge and moderate hydrophobicity are the most critical determinants for the antibacterial activity of AMPs. The majority of cationic AMPs (CAMPs) are short, typically ranging from 5 to 50 amino acid residues, with a tendency to form amphipathic secondary structures upon interaction with bacterial membranes [10, 11]. CAMPs can impair the integrity of bacterial cells through the outer membrane disruption by displacing divalent cations from the lipopolysaccharide (LPS) layer of Gram-negative bacterial cells and/or via direct interaction with the inner membrane, rich in negatively charged phospholipids, phosphatidylglycerol, and cardiolipin, which strongly attract positively charged AMPs [12,13]. For example, Temporin-L a 13 amino acid peptide derived from *Rana temporaria* [14] was reported to induce perturbations of membrane bilayer integrity by interaction with lipid head groups, inducing their tilting, packing defects and membrane thinning [15]. This often be might followed by the formation of peptide-enriched microdomains, allowing the peptide to further diffuse into the inner leaflet of the bilayer by creating “channels” [16]. Besides the aforementioned, some CAMPs (LL-37, BM 22, CM 15 etc.) can also compromise cell integrity through the accumulation of reactive oxygen species (ROS), resulting in the formation of membrane-bound blebs and leakage of cytoplasmic content [17–20]. Irrespective of membrane-damaging activity, some AMPs can enter the cytoplasm and target the key cellular processes, including DNA, RNA, and protein synthesis, and overall, compromise bacterial metabolism [21–23].

Furthermore, in addition to their ability to act independently, CAMPs might synergistically interact with conventional antibiotics, as reported for both Gram-negative and Gram-positive bacteria [24,25]. Synergism can lower the effective concentrations of compounds, thus providing an opportunity to reinforce first-line antibiotics that have already become ineffective [26].

Despite promising antibacterial potential one obvious disadvantage of AMPs lies in their lability towards proteases which is a limiting factor for their therapeutic use. This issue is usually addressed by the integration of unnatural amino acids (including D-enantiomers), cyclization, N- and/or C-terminal modifications of peptide sequences [27,28].

AMPs can be divided into two groups: natural peptides isolated from a variety of organisms, including bacteria, fungi, plants, and animals, and synthetic peptides developed by different approaches, including computer-aided design [27,29].

De novo design of antimicrobial peptides can provide a more versatile approach to develop new antimicrobial agents. It allows to design peptides that have optimized activity, specificity, stability, and other properties. This approach can also lead to the development of entirely new classes of antimicrobial agents, which may be less susceptible to resistance.

In silico de novo design is a less time-consuming and resource-intensive process, but it requires knowledge on structure-activity relationship (SAR) and corresponding predictive models. Many predictive models with high performance have been offered. Despite the improvements in predictive algorithms, most methods share the same conceptual issues. Firstly, during model development, the information on target strains is not taken into account, although the antimicrobial potency of AMPs strongly varies depending on strain-specific bacterial envelope types. Secondly, for model training, most methods use peptides with incomplete or non-existent experiment-based information on their antimicrobial activities [30,31]. Consequently, there is a need to improve available models or develop new ones.

Previously we have performed SAR study using data on AMPs from the Database of Antimicrobial Activity and Structure of Peptides (DBAASP) [32]. The results of the study were target-specific predictive models developed for various targets (including gram-negative *E. coli*) and special tools were introduced into the DBAASP. New CAMPs were designed *de novo* using Antibacterial Peptide Prediction (APP) algorithm of DBAASP. *In vitro* testing revealed high antimicrobial potency and low cytotoxicity of these peptides [33].

In silico designed peptides need additional testing *in vitro* and exploration of their mechanisms of action. In this study, we conducted

Table 1
Minimal inhibitory concentrations (MIC) of antimicrobials against *E. coli* ATCC 25922 at two bacterial concentrations.

Peptide/Antibiotic	Sequence	MIC (μg/mL)	
		5 × 10 ³ CFU/mL	5 × 10 ⁵ CFU/mL
24L	RWIRVWVRKCLR	6.25–12.5	25–50
24D	rwirvwvrkclr	3.125	3.125–6.25
L1L	AIKIRKLFKLLR	12.5	50–100
L1D	aikirklfkllr	3.125–6.25	12.5–25
LCAPL2	GIKIRKLFKLLR	12.5	50
LCAPL4	GIKFFLKLLKKH	50	100
LCAPL8	VARFLKRIIKALF	3.125–6.25	6.25
LCAPL9	GFIKIVRKLRLRF	6.25	6.25
LCAPL10	IIKRILQLKLL	6.25–12.5	25–50
LCAPL14	WKKLKLVWKWKLW	50	100
LCAPL15	KKFLGKWKLRFGW	6.25	12.5
ST1L	LVWKLWVRLRWLK	100	100
ST1D	lvwklwvrlrwlk	25–50	50
Temporin-L	FVQWFSKFLGRIL	>100	>100
Ampicillin	–	6.25–12.5	6.25–12.5
Penicillin G	–	25–50	50
Gentamicin	–	0.78–1.56	3.125–6.25
Kanamycin	–	6.25	6.25
Levofloxacin	–	0.024	0.024
Nalidixic Acid	–	3.125–6.25	3.125–6.25

in vitro testing of *de novo* peptides designed against *E. coli* ATCC 25922. The antibacterial and synergistic properties of peptides, as well as their action on the bacterial cell envelope and intracellular DNA, were evaluated.

2. Materials and Methods

2.1. Materials

Temporin-L was purchased from CRB Discovery; ampicillin sodium salt and kanamycin sulphate were purchased from Carl Roth; 3,6-bis(dimethylamino)-10-nonyl-acridinium bromide (NAO), gentamicin, penicillin G, levofloxacin, nalidixic acid, and Lisogeny-Broth (LB) medium were purchased from Sigma Aldrich. All other reagents were of molecular biology grade.

2.2. Peptide design and synthesis

Peptides were *de novo* designed using the APP tool of DBAASP as described previously [33]. Specifically, CAMPs were predicted to be active against Gram-negative *E. coli* ATCC 25922 using the APP algorithm [34], while the ST1 peptide (L- and D-enantiomers) was designed against both *E. coli* ATCC 25922 and *S. aureus* ATCC 25923. Peptide amino acid sequences are presented in Table 1.

De novo designed peptides were purchased through the custom peptide synthesis service of GenScript Biotech Corporation. All peptides are C-terminally amidated and the labeled versions of 24L, 24D, L1L and L1D have fluorescein isothiocyanate (FITC)-Ahx tag on their N-terminal end. Peptides were delivered as lyophilized materials that had been HPLC-purified and MS-verified (MALDI). All pure peptides were dissolved in sterile ddH₂O to 2 mg/mL stock solutions and stored at -80°C .

2.3. Bacterial strains and plasmids

The bacterial strains used in this study were *E. coli* ATCC 25922 and *E. coli* K12 DH5 α . Plasmid DNA pBbE8k-RFP [35] was a gift from Jay Keasling (Addgene plasmid # 35270; <http://n2t.net/addgene:35270>; RRID:Addgene_35270).

2.4. Minimal inhibitory concentration (MIC) test

Antimicrobial susceptibility testing was carried out using broth microdilution assay, as described before [33]. Briefly, bacteria were grown at 37°C in LB to reach $\text{OD}_{600} = 0.8$. Polypropylene 96-well microtiter plates were used to make twofold serial dilutions of antimicrobials in LB medium ranging from 100 to 0.049 $\mu\text{g/mL}$. Aliquots of 100 μL of bacterial suspension to a final concentration of 5×10^5 colony forming unit (CFU/mL) (standard inoculum size) or 5×10^3 CFU/mL were added to an equal volume of peptide or antibiotic dilutions and the MIC was determined after 16–20 h of incubation at 37°C . The MIC was defined as the minimal concentration of antimicrobial with less than 10% bacterial growth as determined by OD_{600} measurements. Each test was reproduced at least three times.

2.5. MIC test for dividing and non-dividing bacterial cultures

E. coli ATCC 25922 cells from the overnight culture were harvested by centrifugation at 1500g for 5 min. The pellets were washed and resuspended in fresh LB medium (for dividing bacteria experiments) or $1 \times \text{PBS}$ (for non-dividing bacteria experiments) to 10^6 CFU/mL. Aliquots of 100 μL of bacterial suspension were mixed with an equal volume of antimicrobials that had been twofold serially diluted in LB medium (for dividing bacteria) or $1 \times \text{PBS}$ (for non-dividing bacteria) with concentrations ranging from 100 to 1.56 $\mu\text{g/mL}$. All samples were incubated for 1 h at 37°C in a shaking incubator at 1000 rpm and then centrifuged at 1500 g for 5 min to remove antimicrobials. Subsequently, the pellets were resuspended in fresh LB and left at 37°C at 1000 rpm in a shaking incubator. The MIC values were determined as described above. Each test was reproduced at least three times.

2.6. Checkerboard dilution assay for synergy

To evaluate synergistic interactions between CAMPs and antibiotics against *E. coli* ATCC 25922 a checkerboard method was used [36]. Three antibiotics having different mechanisms of action were selected: ampicillin (cell wall synthesis inhibitor), gentamicin (protein synthesis inhibitor), and levofloxacin (DNA gyrase inhibitor). Bacterial culture was grown in LB to the final $\text{OD}_{600} = 0.8$ and resuspended in fresh medium to 10^6 CFU/mL. CAMPs and conventional antibiotics were twofold serially diluted in LB medium in polypropylene 96-well plates to a final volume of 100 μL in each well. Subsequently, bacterial suspension at final concentrations of 5×10^5 CFU/mL or 5×10^3 CFU/mL was applied to each well. The plates were incubated at 37°C in a shaking incubator for 16–20 h at 1000 rpm.

Synergistic interactions between CAMPs and NAO were evaluated against *E. coli* ATCC 25922 at 5×10^5 CFU/mL as described above for CAMPs and antibiotics.

OD_{600} measurements were obtained by reading the samples in a microplate reader.

The fractional inhibitory concentration indices (FICI) were calculated using the following formula:

$\text{FICI} = \text{FIC}_A + \text{FIC}_B = (\text{MIC}_{AB}/\text{MIC}_A) + (\text{MIC}_{BA}/\text{MIC}_B)$, where MIC_A and MIC_B are individual MICs of CAMPs and antibiotics, respectively, and MIC_{AB} and MIC_{BA} are the MICs of CAMPs and antibiotics in combination. The following types of interaction were

defined:

FICI \leq 0.5 (Synergy).

0.5 < FICI \leq 0.625 (Potentiation) 0.625 < FICI \leq 1.0 (Additivity).

1.0 < FICI \leq 4.0 (Indifference) FICI > 4.0 (Antagonism).

Each test was reproduced at least three times.

2.7. Determination of the antimicrobial activity of FITC-labeled CAMPs by microcolony technique

RFP-expressing *E. coli* K12 DH5 α was grown overnight in LB medium supplemented with 0.2% l-arabinose and 50 μ g/mL kanamycin. The overnight culture was diluted 100-fold with fresh LB medium and mixed with 1% low melting point agarose (LMA) at a ratio of 1:3 (v/v). 20 μ L of this suspension was immediately applied onto 1% agarose pre-coated microscope slides, covered with coverslips and left at RT for 5 min to allow agarose to solidify. Coverslips were then removed and twofold serial dilutions of FITC-labeled CAMPs in 1 \times PBS ranging from 100 to 3.125 μ g/mL were pipetted on top of agarose-encapsulated bacterial cells and incubated for 1 h. The slides were rinsed 3 times with 1 \times PBS and left in LB for overnight incubation at 30 $^{\circ}$ C. The formation of microcolonies was observed the following day under Olympus BX41 fluorescence microscope.

2.8. Localization of FITC-labeled CAMPs in the bacterial cell

Bacteria (red fluorescent protein (RFP)-expressing *E. coli* K12 DH5 α or *E. coli* ATCC 25922) were grown overnight in LB medium, encapsulated in 1% LMA (as described above), and incubated with FITC-labeled CAMPs at their MIC concentrations for 1 h on a slide moat at 30 $^{\circ}$ C. The slides were briefly rinsed in 1 \times PBS and observed under Olympus BX41 fluorescence microscope.

To induce the formation of aggregates inside the bacterial cell, *E. coli* ATCC 25922 was grown overnight, diluted 1:100 in fresh LB and incubated at 47 $^{\circ}$ C for 15 min [37]. The cells were then encapsulated in LMA and treated with FITC-labeled CAMPs at their MIC concentrations. The slides were analyzed under Olympus BX41 fluorescence microscope. All the images were captured with CCD camera and processed using FIJI software.

2.9. NAO staining

E. coli ATCC 25222 was grown overnight and diluted with fresh LB medium to final OD₆₀₀=0.5.

Bacteria were then incubated with CAMPs at their $\frac{1}{2}$ MIC concentrations in the presence of NAO at a concentration of 0.235 μ g/mL for 1 h at 37 $^{\circ}$ C with shaking at 1000 rpm. The samples were harvested by centrifugation at 5000g for 3 min. The pellets were washed twice with 1 \times PBS and resuspended in 100 μ L of fresh LB. 5 μ L of the resulting suspension was spotted onto 1% agarose pre-coated microscope slides, covered with coverslips and examined under Olympus BX41 fluorescence microscope. Images were captured and processed as described above.

2.10. Quantification of blebbed bacterial cells

RFP-expressing *E. coli* K12 DH5 α was grown and encapsulated in LMA as described above. The slides were washed in 1 \times PBS and incubated at room temperature (RT) for 30 min to remove the traces of medium. Subsequently, the slides were placed onto a slide moat, and CAMPs (in the presence or absence of 100 mM thiourea (TU)) diluted in 1 \times PBS to their $\frac{1}{2}$ MIC concentrations, were added to agarose-encapsulated bacterial cells and left at 30 $^{\circ}$ C for 10 min. The slides were then washed in 1 \times PBS for 30 min and observed under Olympus BX41 fluorescence microscope. The percentage of blebbed cells was determined by counting 50 cells on each slide. Each test was reproduced at least three times. Statistical significance between groups was determined by two-tailed, unpaired Student's T-Test.

2.11. Determination of CAMP-DNA interactions by electro mobility shift assay (EMSA)

Plasmid DNA pUC18 (600 ng) in 10 mM Tris-HCl buffer (pH 7.4) was mixed with CAMPs at a molar ratio of 1:1000 or 1:500 to a final volume of 60 μ L and incubated at 37 $^{\circ}$ C for 1 h. Subsequently, 6 \times loading buffer (30% glycerol, 1 mM EDTA, 0.25% bromophenol) was added and aliquots of 15 μ L were loaded into 1% agarose gel. The gel was run in 1 \times Tris-acetate-EDTA buffer (40 mM Tris, 20 mM acetic acid, 1 mM EDTA) at 0.6 V/cm.

The gel was stained with ethidium bromide and visualized under ultraviolet illumination. Only peptides showing full retardation of plasmid DNA at 1:1000 DNA:CAMP molar ratio were tested at a molar ratio of 1:500.

2.12. Determination of DNA double-strand breaks (DSBs) by pulsed-field gel electrophoresis (PFGE)

A fresh bacterial culture of *E. coli* ATCC 25922 in LB (OD₆₀₀ = 0.8) was pelleted at 1500 rpm for 5 min and diluted in 1 \times PBS to 1.5 \times 10⁹ CFU/mL. The bacterial suspension was then mixed with 1.5% LMA at a ratio of 1:2 and approximately 80 μ L of the solution was dispensed into each slot of a plastic plug mold (Bio-Rad) and left to solidify at RT. The blocks containing bacterial cells were then transferred into 2 mL tubes (one block per tube) containing 500 μ L of solutions of peptides (100 μ g/mL), levofloxacin (0.5 μ g/mL), or ampicillin (50 μ g/mL) in 1 \times PBS and incubated at 37 $^{\circ}$ C for 2 h (peptides and ampicillin) or 1 h (levofloxacin) in the presence or

absence of 100 mM TU without agitation. Following the exposure to antimicrobial agents, the solutions were removed and the blocks were treated with proteinase K (1 mg/mL) in digestion buffer (100 mM EDTA, 50 mM Tris-HCl, 1% sodium lauryl sarcosine, pH 8) and incubated overnight at 50 °C without agitation. The blocks were then washed 4 × 45 min in 1 × TE (10 mM Tris-HCl, 10 mM EDTA, pH 8.0) and stored at 4 °C in TE buffer until PFGE. The plugs containing bacterial chromosomal DNA were loaded into wells of 1% agarose gel. Electrophoresis was run in 0.5 × TBE buffer (45 mM TRIS, 45 mM boric acid, 1.0 mM EDTA, pH 8.3) at 300 V for 6 h at 12 °C with a pulse time of 25 s using Gene Navigator Pulsed Field Gel Electrophoresis System (Amersham Biosciences). The gel was stained with ethidium bromide and visualized under ultraviolet illumination.

3. Results

3.1. Antimicrobial susceptibility testing

The MICs of 10 *de novo* designed CAMPs, D-enantiomers of three of these CAMPs (24L, L1 and ST1L), 6 commercially available antibiotics (ampicillin, kanamycin, levofloxacin, penicillin G, nalidixic acid, gentamicin) and Temporin-L (a natural AMP, sharing some similarities with our *de novo* peptides in terms of cationicity, the number of amino acids and linearity) [15,16] were determined for two bacterial inoculum densities (5×10^5 and 5×10^3 CFU/mL) of *E. coli* ATCC 25922 in LB medium.

A 4-fold or greater change in the MIC of antimicrobials resulting from a 100-fold change in bacterial concentration was considered as an inoculum effect [38,39]. At lower cell densities compared to a standard inoculum density of 5×10^5 CFU/mL, only the MIC of peptide L1L decreased 8-fold, while most of the tested CAMPs showed 2- to 4-fold decrease in their MIC values. In contrast, the MIC values of only one from 6 tested antibiotics (gentamicin) changed in response to the changes in the bacterial concentration (see Table 1). Surprisingly, Temporin-L did not show antimicrobial activity at any tested concentrations at either inoculum density.

Since there is plenty of data reporting that bacterial susceptibility toward antimicrobial agents might depend on the metabolic state of a bacterial culture [40,41], we decided to assess the MIC values of Temporin-L and *de novo* designed CAMPs against dividing and non-dividing cells of *E. coli* ATCC 25922. In this set of experiments, overnight culture of bacteria was pre-incubated with CAMPs in 1 × PBS or LB for 1 h at 37 °C and recovered in fresh medium overnight.

As shown in Table 2, at a standard inoculum density, MIC values against dividing and non-dividing cells were not significantly different for the majority of the tested CAMPs. However, in 1 × PBS, MIC values markedly decreased for LCAPL14 (>32-fold) and Temporin-L (being inactive in LB) exhibited antimicrobial activity at 12.5–25 µg/mL. The revival of the antimicrobial properties of Temporin-L in 1xPBS might most probably be attributed to its antagonistic interactions with some components of the LB. The obtained results indicate that all the tested *de novo* CAMPs retain their antibacterial activity regardless of the metabolic state of bacteria. Also, our MIC experiments unravel that, in contrast to conventional antibiotics, the antimicrobial activity of CAMPs did not significantly differ between 1 h and overnight incubation in LB medium (compare Tables 1 and 2).

3.2. Synergy between CAMPs and conventional antibiotics

Synergy analysis between 11 *de novo* CAMPs and 3 conventional antibiotics was performed against *E. coli* ATCC 25922 at two bacterial inoculum densities using a checkerboard assay. At a standard cell density, peptides 24L, L1L, and L1D showed synergistic effects with all the tested antibiotics (Fig. 1 and Table 3). The highest number of synergistic combinations were obtained for gentamicin, which, apart from 24L, L1L, and L1D, showed synergy with LCAPL2 and LCAPL10. In all synergistic combinations, the MICs of CAMPs decreased 4 times, while the MIC values of some antibiotics decreased more significantly, for example, the MIC value of

Table 2
Minimal inhibitory concentrations (MIC) of antimicrobials against dividing (LB) and non-dividing (PBS) cells of *E. coli* ATCC 25922. Bacterial cell density – 5×10^5 CFU/mL.

Antibiotic/Peptide	MIC (µg/mL)	
	PBS	LB
Ampicillin	>100	>100
Gentamicin	25	50
24L	≥100	50–100
24D	25–50	12.5
L1L	12.5	50–100
L1D	12.5–25	12.5
LCAPL2	12.5–25	50
LCAPL4	50–100	≥100
LCAPL8	6.25	6.25
LCAPL9	1.56	6.25
LCAPL10	12.5	25–50
LCAPL14	1.56	50–100
LCAPL15	12.5	12.5–25
ST1L	≥100	≥100
ST1D	50	50
Temporin-L	12.5–25	>100

gentamicin in combination with L1D decreased 16-fold. At 5×10^3 CFU/mL, synergy was observed only in combination with ampicillin for two CAMPs (LCAPL2 and ST1L) with the 8-fold decreased MICs of both antimicrobial agents.

At both inoculum densities, peptide-antibiotic combinations with FICI values of $0.5 < \text{FICI} \leq 0.625$ were labeled as potentiation. The maximum decrease in peptide MIC (16-fold) was observed for LCAPL15 in combination with ampicillin at a standard inoculum density, while the rest of the CAMPs showed a less significant decrease in their MIC values (2–8 fold). The changes of the MIC values of ampicillin were mostly in the same range as those of CAMPs, however, levofloxacin and gentamicin showed a more prominent decrease in their MICs. For example, the MIC of levofloxacin decreased 32-fold in combinations with LCAPL2 and LCAPL10 at 5×10^3 CFU/mL and 5×10^5 CFU/mL, respectively, while the maximum (64-fold) decrease of MIC was revealed for gentamicin in combinations with ST1D and ST1L at 5×10^3 CFU/mL and 5×10^5 CFU/mL, respectively. No antagonistic interactions were observed in any antibiotic-peptide combinations.

3.3. CAMP localization in live bacterial cells

To study the mechanisms of action, we selected 4 *de novo* designed CAMPs, of which 3 (L1L, 24L, and L1D) showed synergy with all tested antibiotics, while 24D is the enantiomer of 24L.

We also intended to study the mechanism of action of ST-1L (predicted to be active against *E. coli* and *S. aureus* and showing synergy with ampicillin) and its enantiomer ST-1D, unfortunately, labeling of these peptides with FITC completely abolished their antimicrobial activity, therefore we were unable to include them in these studies.

Prior to the investigation of peptide localization in the bacterial cell, effective concentrations of the selected FITC-labeled CAMPs were determined using the microcolony technique. Multiple microcolonies were observed for FITC-24L, FITC-24D, and FITC-L1L at

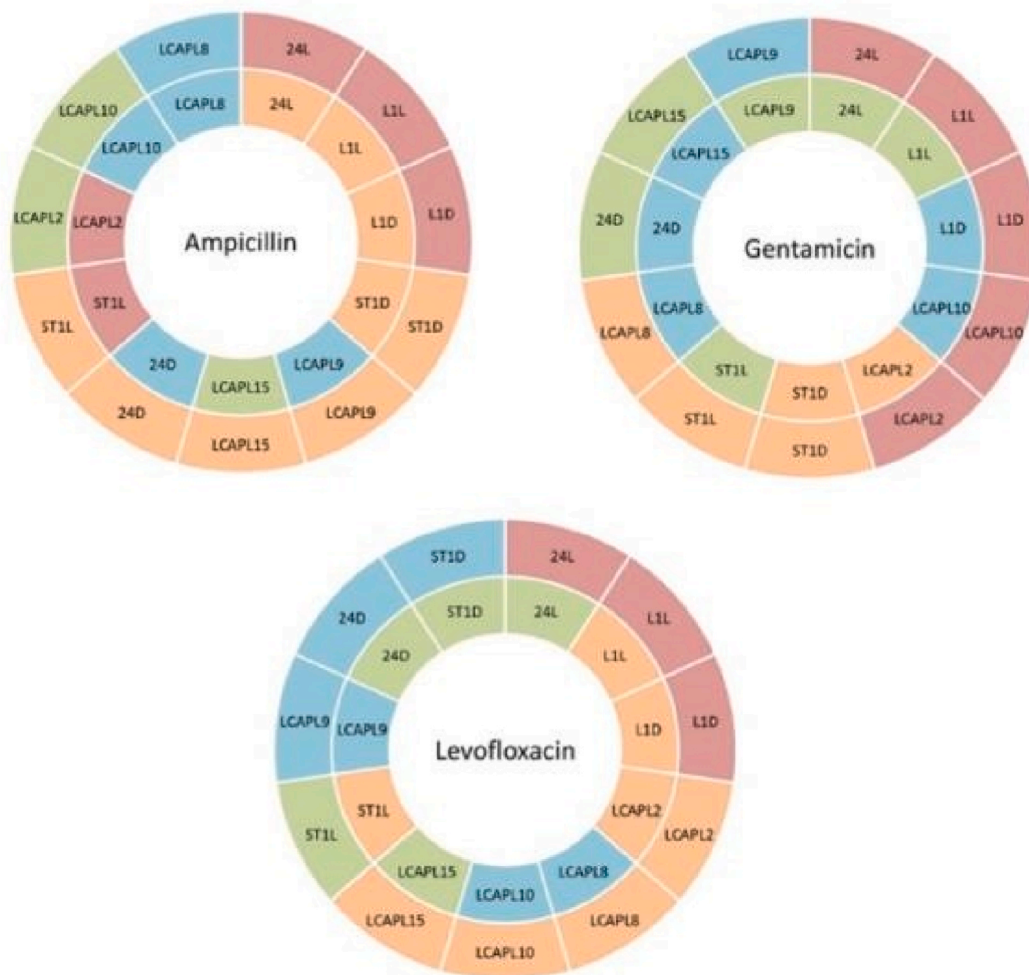


Fig. 1. Synergistic interactions between peptides and antibiotics against *E. coli* ATCC 25922 at two bacterial concentrations. Inner circle – 5×10^3 CFU/mL, outer circle – 5×10^5 CFU/mL; Colors: blue– indifference; green – additivity; orange – potentiation; pink – synergy.

Table 3

Synergistic interactions between peptides and antibiotics against *E. coli* ATCC 25922 at two bacterial concentrations. MIC_A – MIC of peptide alone; MIC_B – MIC of antibiotic alone; MIC_{AB} – MIC of peptide in combination with antibiotic; MIC_{BA} – MIC of antibiotic in combination with peptide; FICI – fractional inhibitory concentration index.

Peptides	5 × 10 ³ CFU/mL					5 × 10 ⁵ CFU/mL				
	MIC (A)	MIC (B)	MIC (AB)	MIC (BA)	FICI	MIC (A)	MIC (B)	MIC (AB)	MIC (BA)	FICI
Ampicillin										
24L	12.5	6.25	6.25	0.78	0.625	25	12.5	6.25	3.125	0.5
24D	3.125	12.5	3.125	0.195	1.016	6.25	12.5	3.125	1.56	0.625
L1L	12.5	6.25	6.25	0.39	0.563	50	12.5	12.5	3.125	0.5
L1D	3.125	12.5	1.56	1.56	0.625	12.5	12.5	3.125	3.125	0.5
LCAPL2	12.5	6.25	3.125	1.56	0.5	50	12.5	25	3.125	0.75
LCAPL8	6.25	12.5	6.25	0.195	1.016	6.25	6.25	6.25	0.195	1.031
LCAPL9	6.25	6.25	6.25	0.098	1.016	6.25	12.5	3.125	1.56	0.625
LCAPL10	6.25	6.25	6.25	0.098	1.016	25	6.25	12.5	1.56	0.75
LCAPL15	6.25	12.5	3.125	3.125	0.75	12.5	6.25	0.78	3.125	0.563
ST1L	100	6.25	25	0.78	0.375	100	12.5	50	1.56	0.625
ST1D	25	6.25	3.125	3.125	0.625	50	12.5	25	1.56	0.625
Gentamicin										
24L	12.5	1.56	6.25	0.78	1	50	3.125	12.5	0.78	0.5
24D	3.125	1.56	3.125	0.024	1.015	6.25	3.125	3.125	1.56	1
L1L	12.5	1.56	6.25	0.39	0.75	50	3.125	12.5	0.78	0.5
L1D	3.125	1.56	3.125	0.195	1.125	25	6.25	6.25	0.39	0.313
LCAPL2	12.5	1.56	6.25	0.195	0.625	50	6.25	12.5	0.78	0.375
LCAPL8	3.125	0.78	3.125	0.024	1.031	6.25	3.125	3.125	0.098	0.531
LCAPL9	6.25	0.78	3.125	0.39	1	6.25	3.125	6.25	0.098	1.031
LCAPL10	12.5	1.56	12.5	0.195	1.125	50	3.125	12.5	0.78	0.5
LCAPL15	6.25	0.78	6.25	0.024	1.031	12.5	3.125	3.125	1.56	0.75
ST1L	100	1.56	50	0.78	1	100	3.125	50	0.049	0.516
ST1D	50	1.56	25	0.024	0.516	50	3.125	6.25	1.56	0.625
Levofloxacin										
24L	6.25	0.024	3.125	0.006	0.75	25	0.024	6.25	0.006	0.5
24D	3.125	0.024	1.56	0.012	1	3.125	0.024	3.125	0.001	1.031
L1L	12.5	0.024	6.25	0.003	0.625	100	0.024	25	0.006	0.5
L1D	6.25	0.024	3.125	0.002	0.563	25	0.024	6.25	0.003	0.375
LCAPL2	12.5	0.024	6.25	0.001	0.531	50	0.024	25	0.003	0.625
LCAPL8	3.125	0.024	3.125	0.006	1.25	6.25	0.024	3.125	0.003	0.625
LCAPL9	6.25	0.024	6.25	0.024	2	6.25	0.024	6.25	0.006	1.25
LCAPL10	12.5	0.024	12.5	0.001	1.031	25	0.024	12.5	0.001	0.531
LCAPL15	6.25	0.024	1.56	0.012	0.75	12.5	0.024	6.25	0.002	0.563
ST1L	100	0.024	12.5	0.012	0.625	100	0.024	25	0.012	0.75
ST1D	50	0.024	25	0.012	1	50	0.024	50	0.001	1.031

concentrations lower than 25 µg/mL, while for FITC-L1D, the colonies appeared at concentrations lower than 12.5 µg/mL. Thus, 25 µg/mL or 12.5 µg/mL were considered as their MIC values in this system and were used for the evaluation of CAMP localization patterns in live bacteria.

The treatment of *E. coli* ATCC 25922 with FITC-labeled CAMPs showed that the FITC signal was localized predominantly along the membrane surface of treated cells with slightly enhanced fluorescence at the bacterial poles and septal regions (Fig. 2A). Similar results were obtained for *E. coli* K12 DH5α (data not shown). A different distribution pattern of CAMPs was observed for RFP-expressing *E. coli* K12 DH5α (bearing inclusion bodies (IB) Fig. 2B), where, as shown in Fig. 2C, FITC signal was predominantly localized in IBs. IBs are submicron proteinaceous aggregates (usually ranging from 50 to 800 nm), accumulated in cells as a result of stress or overexpression of recombinant proteins [42,43]. Under bright field microscope, IBs are visualized as dense dark areas in the cytoplasm at the poles and septal regions [42].

To define whether the accumulation of CAMPs in IBs could be attributed to the presence of recombinant proteins or caused by the attraction and accumulation of CAMPs by endogenously produced protein aggregates, we subjected *E. coli* K12 DH5α to heat shock at 47 °C. As shown in Fig. 2D, heat shock promoted the generation of multiple aggregates inside the bacterial cells and the localization of FITC-labeled CAMPs corresponded to the exact location of these aggregates.

3.4. The action of CAMPs on anionic lipid distribution in live bacteria

NAO is known to specifically bind to anionic phospholipids (preferentially cardiolipin) by an interaction between its quaternary amine and the phosphate residue of the phospholipids and by an intercalation of its hydrophobic acridine moiety into the lipid bilayer [44,45].

Before NAO staining experiments, the MIC of NAO against *E. coli* ATCC 25922 was determined. An antibacterial effect of NAO was detected at 3.125 µg/mL, thus a 13-fold lower concentration in subsequent experiments was used. In our experiments, untreated

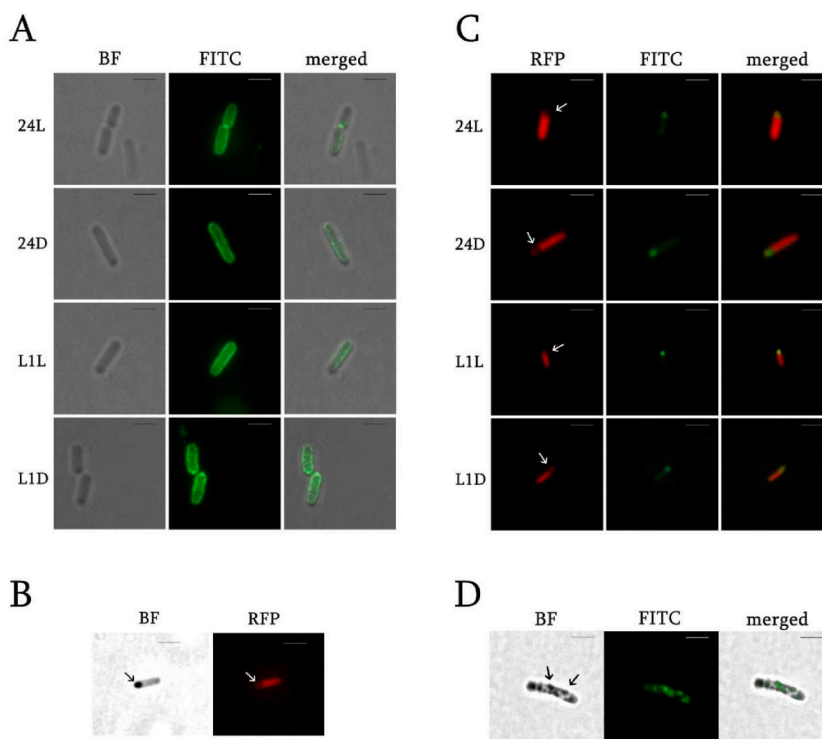


Fig. 2. Presence or absence of IBs results in the different distribution patterns of FITC-labeled CAMPs in *E. coli* cells. (A) Representative images of LMA-encapsulated *E. coli* ATCC 25922 cells treated with FITC-labeled CAMPs at their MIC concentrations (as described in Materials and Methods). (B) Bright field and fluorescent images of RFP-expressing *E. coli* K12 DH5 α cells bearing IBs. (C) Representative images of LMA-encapsulated RFP-expressing *E. coli* K12 DH5 α cells treated with FITC-labeled CAMPs at their MIC concentrations. (D) Representative images of heat-shocked *E. coli* DH5 α cells treated with FITC-labeled peptide 24D. All images were captured with CCD camera of Olympus fluorescent microscope equipped with 100 \times oil-immersion objective lens. Scale bar – 2 μ m. Arrows are pointing at IBs.

bacterial cells had an NAO-staining pattern similar to what we had observed in *E. coli* ATCC 25922 cells treated with FITC- labeled CAMPs. However, non-fluorescent CAMPs and Temporin-L at their $\frac{1}{2}$ MIC concentrations induced a significant redistribution of anionic phospholipids observed as discrete green fluorescent domains along the bacterial cell envelope (Fig. 3A). Interestingly, when incubated with RFP-expressing *E. coli* cells, NAO was predominantly localized in IBs as it was observed for FITC-labeled CAMPs (Fig. 3B). Overall, the cells treated with CAMPs were characterized by brighter staining due to better NAO uptake. These results led to the investigation of a potential synergy between NAO and CAMPs. As shown in Fig. 3C, NAO indeed exhibited synergy when in combination with 24L, L1L and L1D. Also, we noticed that all the tested CAMPs induced blebbing with intense NAO fluorescence at bleb origination sites (Fig. 3D).

3.5. Antimicrobial peptide treatment promotes blebbing and inner membrane perturbations in *E. coli* cells

Since bacterial blebs detach from the cell surface in a time-dependent manner, bacterial cells were immobilized by encapsulating in LMA (as described in the Materials and Methods section). This approach allows newly formed vesicles to remain in the vicinity of the bacterial cells even after detachment. For these experiments, *E. coli* K12 DH5 α with a cytoplasmic expression of RFP was used. Therefore, vesicles (if any) produced as a result of inner membrane disruption could be detected under a fluorescent microscope as the red fluorescence of cytoplasmic RFP leaked into vesicles. As shown in Fig. 4 A,B, all the tested CAMPs (L1L, L1D, 24L and 24D) and Temporin-L induced blebs with strong red fluorescence. The maximum percentage of blebbed cells –53% was observed for L1D, while the minimum – 12%, was observed for Temporin-L. In untreated cells, the percentage of blebbed cells never exceeded 1%. Blebbing was accompanied with the overall decreased fluorescence intensity of *E. coli* cells pointing to the leakage of cytoplasmic content. In order to test whether ROS was involved in the generation of blebs, bacterial cells were treated with CAMPs in the presence of TU, which is known to possess a radical scavenging activity [46]. As shown in Fig. 4A, TU significantly reduced the percentage of blebbed cells for all the tested CAMPs but not for Temporin-L.

3.6. Interaction of peptides with the plasmid DNA

Since recent evidence suggests that CAMPs have a multi-target mechanism of action [47] and can interact with multiple anionic

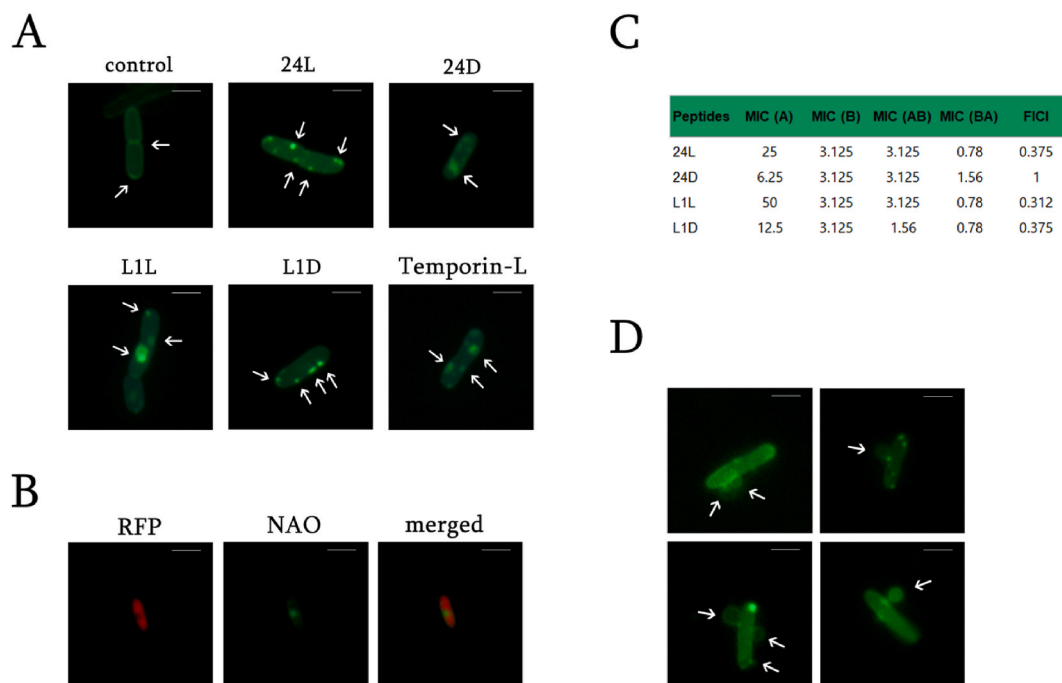


Fig. 3. CAMPs induce the redistribution of negatively charged phospholipids in *E. coli* cells. (A) Representative images of *E. coli* ATCC 25922 cells treated with NAO alone (control) or in combination with CAMPs at their $\frac{1}{2}$ MIC. Arrows are pointing at NAO accumulation sites. (B) Representative images of NAO distribution in RFP-expressing *E. coli* K12 DH5 α cells. (C) Synergy analysis against *E. coli* ATCC 25922 between CAMPs and NAO was performed by checkerboard method. MIC_A and MIC_B are the individual MICs of CAMPs and NAO, respectively, and MIC_{AB} and MIC_{BA} are the MICs of CAMPs and NAO in combination respectively. (D) Representative images of CAMP-induced blebbing of *E. coli* ATCC 25922 cells stained with NAO. Arrows pointing at bleb origination sites. All images were captured with CCD camera of Olympus fluorescent microscope equipped with 100 \times oil-immersion objective lens. Scale bar – 2 μ m.

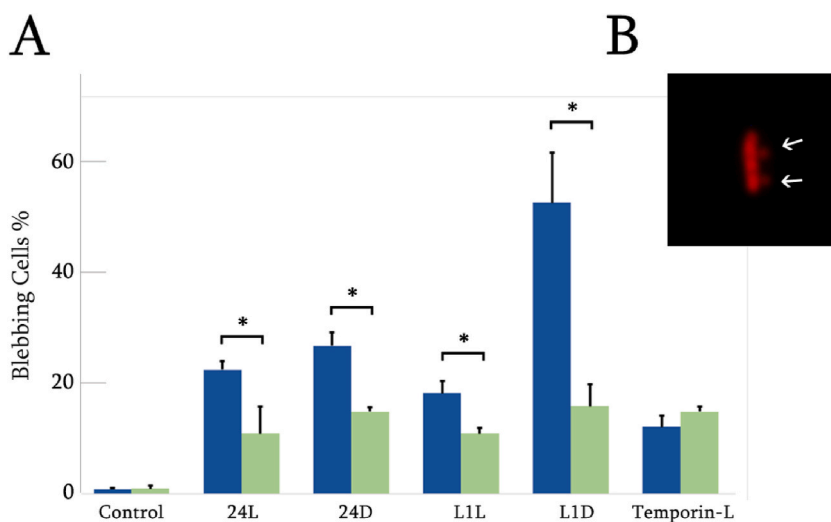


Fig. 4. CAMPs promote ROS-dependent blebbing of RFP-expressing *E. coli* K12 DH5 α cells, accompanied by the leakage of cytoplasmic content. (A) Percentage of blebbed cells after 10 min treatment with CAMPs or Temporin-L in the absence (blue columns) or presence (green columns) of TU. The results are the means of at least 3 independent experiments. Error bars indicate the standard error of the mean. * ($p < 0.05$). (B) Representative image of blebbed RFP-expressing *E. coli* K12 DH5 α cells.

targets, such as DNA [21,48–50], we examined the ability of *de novo* CAMPs to interact with DNA by employing EMSA. As shown in Table 4, peptides 24L, 24D, and L1L completely inhibited the migration of pUC18 plasmid DNA through the agarose gel at a molar ratio of 1:1000, while at a molar ratio of 1:500, these AMPs only partially retarded DNA migration. The majority of the rest of the CAMPs

partially retarded DNA migration through the gel at a molar ratio of 1:1000.

3.7. CAMPs induce DSB formation in *E. coli* genomic DNA

To study the ability of CAMPs to induce DSBs in bacterial genomic DNA, we selected CAMPs with different DNA-binding properties. Live *E. coli* ATCC 25922 cells encapsulated in 1% LMA blocks were treated with peptides (24L, 24D, L1L, L1D, ST1L, LCAPL2, and LCAPL8) or conventional antibiotics (levofloxacin and ampicillin) as described in the Materials and Methods section. As shown in Fig. 5A, the pattern of background DNA damage in the cells treated with ampicillin did not differ from that of control samples, however, levofloxacin induced the generation of DNA fragments of approximately 50 kbp. A similar but less intense DNA damage pattern was noticed for peptides 24L, L1D, and ST1L. For 24D, L1L, LCAPL2, and LCAPL8 ~50 kbp fragments were barely detected. To determine whether the generation of ROS was responsible for observed DSB formation, we compared DNA fragmentation patterns of CAMP-treated samples in the presence or absence of TU. As depicted in Fig. 5B, TU did not significantly affect the formation of DNA fragments.

4. Discussion

Our antimicrobial susceptibility testing experiments are in line with the previously described phenomenon that AMPs are fast-acting agents and that their antibacterial activity is not dramatically affected by either low bacterial cell densities (below 5×10^5 CFU/mL) [51] or the ability of bacteria to divide [40,52].

Numerous papers described the ability of AMPs to synergize with conventional antibiotics [23,24,53], however, to the best of our knowledge, there are no studies describing the effect of bacterial inoculum density on the combinatorial activity of both types of antimicrobials. In our study, a checkerboard assay between CAMPs and selected antibiotics was performed for standard (5×10^5 CFU/mL) and 100 times lower inoculum densities.

Most of the synergistic interactions were observed for a cell density of 5×10^5 CFU/mL, while at 5×10^3 CFU/mL, synergy was only observed for ampicillin in combination with LCAPL2 or ST1L. This may be explained by the better individual performance of antimicrobials at a lower cell density, resulting in increased FICI values. On the other hand, 24L, L1L, and L1D have shown synergy with all the tested antibiotics at a standard inoculum density, suggesting that these CAMPs might possess similar modes of action, most probably involving the disruption of bacterial cell envelope, making it easier for antibiotics to reach their targets. This assumption is in line with our finding that, out of 22 peptide-antibiotic combinations that showed a potentiation effect, in about 82% of cases, the activity of the antibiotic was potentiated by the peptide. Interestingly, all tested CAMPs showed the ability to potentiate an antibiotic in at least one combination. Earlier the potentiating properties of antimicrobial peptides were reported for several peptide/peptidomimetic-antibiotic combinations (e.g. a combination of daptomycin with ampicillin) [53,54]. Therefore, it can be concluded that *de novo* peptides used in this work have the potential to enhance the activity of ampicillin, gentamicin, and levofloxacin against *E. coli* ATCC 25922 strain depending on particular favorable conditions, such as bacterial cell density.

In order to investigate the mechanism of action of CAMPs on the bacterial envelope, we selected 4 CAMPs (L1L, L1D, 24L, and 24D), 3 of which have revealed a synergy with all the tested antibiotics at a standard inoculum density. Our microscopy studies have shown that all the tested FITC-labeled CAMPs and NAO have a similar staining pattern with preferential localization on the bacterial cell surface with slightly more enhanced fluorescence in the regions of bacterial poles and septa that are characterized by an abundance of anionic charge. However, after simultaneous treatment with NAO and CAMPs, the redistribution of anionic phospholipid domains was noticed. These observations are in line with previous studies [55–57]. Since it was shown that NAO acts synergistically with CAMPs, the lipid redistribution pattern cannot be solely attributed to CAMPs. Also, the observed synergy between NAO and CAMPs provides an explanation for the enhanced NAO fluorescence intensity when administered in combination with peptides. The possible mechanism

Table 4
Electro mobility shift assay (EMSA) results of CAMPs at two different DNA: peptide molar ratios. F – full retardation; P – partial retardation; N – no retardation.

Peptides	DNA: Peptide	
	1:1000	1:500
24L	F	P
24D	F	P
L1L	F	P
L1D	P	–
LCAPL2	P	–
LCAPL4	N	–
LCAPL8	P	–
LCAPL9	P	–
LCAPL10	P	–
LCAPL14	P	–
LCAPL15	P	–
ST1L	P	–

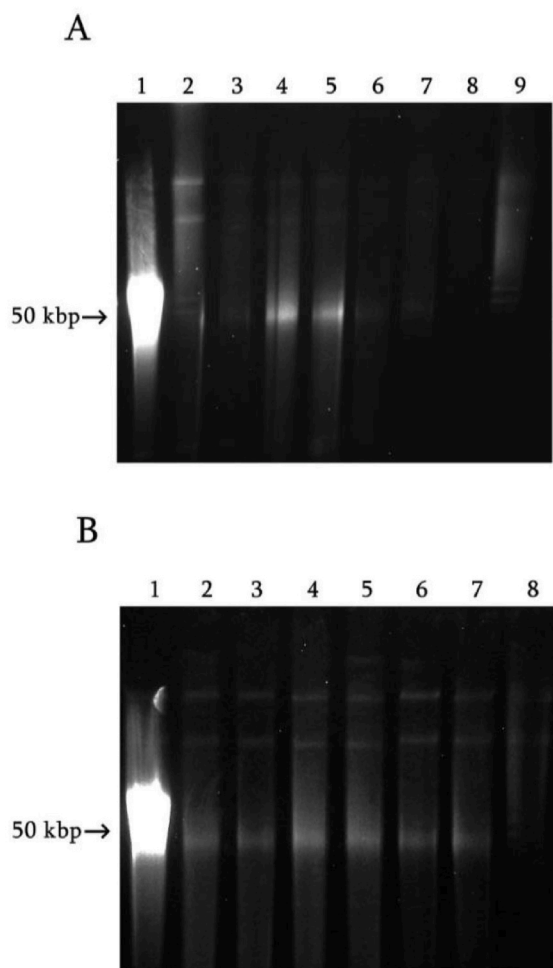


Fig. 5. CAMPs induce ROS-independent DSBs in genomic DNA of *E. coli* ATCC 25922. (A) LMA-encapsulated cells were treated with CAMPs (100 $\mu\text{g}/\text{mL}$), levofloxacin (0.5 $\mu\text{g}/\text{mL}$), or ampicillin (50 $\mu\text{g}/\text{mL}$) (see Materials and Methods section) and DSB formation was monitored using PFGE. Lane 1 – levofloxacin; Lane 2 – ampicillin; Lane 3 – L1L; Lane 4 – L1D; Lane 5–24L; Lane 6–24D; Lane 7 – LCAPL2; Lane 8 – LCAPL8; Lane 9 – untreated cells; (B) LMA-encapsulated cells were treated with peptides 24L, L1D, and ST1 in the absence (lanes 2, 4, and 6) or presence (lanes 3, 5, and 7) of 100 mM TU. Lane 1 and Lane 8 show levofloxacin and untreated cells, respectively. For full images please see Supplemental Material.

might involve CAMP-induced permeabilization of the bacterial outer membrane. This, in turn, could lead to improved accessibility of NAO to its target in the bacterial inner membrane.

In order to study the impact of CAMPs on bacterial inner membrane, we conducted experiments on RFP-expressing *E. coli* K12 DH5 α . These studies further confirmed the inner membrane perturbing properties of CAMPs. We showed that all the tested CAMPs as well as Temporin-L induce formation of blebs and vesicles with intense RFP fluorescence, thus proving dramatic perturbations in the inner membrane of treated cells. Bacterial cell blebbing was previously described for several natural antimicrobial peptides [20,58]. For example, synthetic cathelicidin BM 22 was reported to induce the generation of reactive oxygen species by disrupting the membrane-bound aerobic respiratory electron transport chain leading to the accumulation of ROS and bleb formation. ROS scavenger TU reduced cellular ROS levels and overcame these bactericidal effects [20]. In our experiments, treatment with TU resulted in the significant change of percentage of blebbed cells for all the tested CAMPs. However, in the case of Temporin-L, TU did not affect the reduction of blebbed cell counts. The observations that TU did not fully reverse CAMP-induced blebbing and that Temporin-L-induced blebbing was not affected by the presence of TU probably indicate that some other mechanisms (other than ROS) might also be involved in this process.

We also showed that IBs (if present in bacterial cells) represent the main localization sites for CAMPs. Since IBs are localized in the proximity of the regions with altered membrane curvature [59,60] the uptake of CAMPs might be easier at these specific sites, allowing IBs to absorb harmful substances (peptides, in this case) and lower their overall concentration for the rest of the cells thus promoting their survival. Indeed, recent reports suggest that protein aggregates help bacteria to cope with proteotoxic stresses and improve survival during antibiotic exposure [37,61]. Further research is needed to understand the mechanisms and outcomes IB-CAMPs

interactions.

In addition to causing destruction of bacterial cell morphology and eventual cell death, numerous studies have also reported that AMPs provoke DNA damage in bacterial cells [62,63]. In our experiments several CAMPs were shown to induce DSBs in bacterial chromosomal DNA, resulting in the formation of DNA fragments of the similar length as those produced by gyrase inhibitor levofloxacin [64]. However, the generation of ~50 kbp DNA fragments was not affected by the presence of TU and, also, it did not show any correlation with the ability of CAMPs to form complexes with DNA. Our results propose that the DSBs are neither a result of a direct peptide- DNA interaction nor the consequence of ROS. Instead, the observed DSB formation may be due to the impaired osmoregulatory capacity of *E. coli* cells, resulting in structural changes to the genome that hinder DNA replication [65] in a manner similar to the mechanism of action of the replication-targeting antibiotic levofloxacin [64].

In this study we evaluated antimicrobial potencies of D enantiomers of three CAMPs 24L, L1L, and ST1L. D variants of all three CAMPs have shown higher antibacterial performance regardless bacterial density and metabolic state of bacteria. Also the substitution of L-amino acids with their D-variants effected the ability of CAMPs to synergize with antibiotics and induce genomic DNA damage in *E. coli* cells. For example out of 3 CAMPs exhibiting synergistic interactions with antibiotics, D enantiomer of only one CAMP - L1L retained the property to synergize with antibiotics. Also differences between enantiomers were noticed in their ability to induce genomic fragmentation in *E. coli* cells (DNA damage was observed for 24L and L1D but not for 24D and L1L). It is well established that substitution of L-amino acids with their D – counterparts protects CAMPs from protease degradation [28,33], however in our studies only the enhanced antibacterial activity of D-enantiomers, but not their ability to synergize with antibiotics and induce DNA damage, can be easily attributed to their stability towards proteases.

Overall, our data indicate that all *de novo* CAMPs used in this study are able to potentiate antibiotics probably through the destabilization of bacterial envelope. Together with membrane disruptive properties, *de novo* CAMPs could also promote genomic DNA fragmentation. These findings contribute to a better understanding of the unique properties of CAMPs.

Data availability

All data is included in the manuscript.

CRedit authorship contribution statement

Margarita Karapetian: Writing – review & editing, Writing – original draft, Investigation, Funding acquisition, Formal analysis. **Evgenia Alimbarashvili:** Writing – review & editing, Writing – original draft, Investigation, Formal analysis. **Boris Vishnepolsky:** Software, Formal analysis, Data curation. **Andrei Gabrielian:** Funding acquisition. **Alex Rosenthal:** Funding acquisition. **Darrell E. Hurt:** Funding acquisition. **Michael Tartakovsky:** Funding acquisition. **Mariam Mchedlishvili:** Investigation. **Davit Arsenadze:** Investigation. **Malak Pirtskhalava:** Writing – review & editing, Supervision, Funding acquisition, Conceptualization. **Giorgi Zaalishvili:** Writing – review & editing, Writing – original draft, Visualization, Supervision, Methodology, Formal analysis, Data curation, Conceptualization.

Declaration of competing interest

The authors declare that they have no known competing financial interests or personal relationships that could have appeared to influence the work reported in this paper.

Acknowledgements

This research was funded by the International Science and Technology Center, Kazakhstan [G-2102].

M.K. was supported by PhD research grant from Shota Rustaveli National Science Foundation of Georgia [PHDF-21-859].

We thank Knowledge Fund for covering publishing fees.

We thank Dr. Elisabed Zaldastanishvili for reading the manuscript and valuable comments and Sophiko Tsikarishvili for the artwork.

Appendix A. Supplementary data

Supplementary data to this article can be found online at <https://doi.org/10.1016/j.heliyon.2024.e27852>.

References

- [1] P. Cardoso, H. Glossop, T.G. Meikle, A. Aburto-Medina, C.E. Conn, V. Sarojini, C. Valery, Molecular engineering of antimicrobial peptides: microbial targets, peptide motifs and translation opportunities, *Biophys Rev* 13 (2021) 35–69, <https://doi.org/10.1007/s12551-021-00784-y/Published>.
- [2] Antimicrobial Resistance Collaborators, Global burden of bacterial antimicrobial resistance in 2019: a systematic analysis, *Lancet* 399 (2022) 629–655, [https://doi.org/10.1016/S0140-6736\(21\)02724-0](https://doi.org/10.1016/S0140-6736(21)02724-0).

- [3] Z. Breijyeh, B. Jubeh, R. Karaman, Resistance of gram-negative bacteria to current antibacterial agents and approaches to resolve it, *Molecules* 25 (2020), <https://doi.org/10.3390/molecules25061340>.
- [4] C. Ghosh, P. Sarkar, R. Issa, J. Haldar, Alternatives to conventional antibiotics in the era of antimicrobial resistance, *Trends Microbiol.* 27 (2019) 323–338, <https://doi.org/10.1016/j.tim.2018.12.010>.
- [5] Y. Liu, J. Shi, Z. Tong, Y. Jia, B. Yang, Z. Wang, The revitalization of antimicrobial peptides in the resistance era, *Pharmacol. Res.* 163 (2021), <https://doi.org/10.1016/j.phrs.2020.105276>.
- [6] R. Rathinakumar, W.F. Walkenhorst, W.C. Wimley, Broad-spectrum antimicrobial peptides by rational combinatorial design and high-throughput screening: the importance of interfacial activity, *J. Am. Chem. Soc.* 131 (2009) 7609–7617, <https://doi.org/10.1021/ja8093247>.
- [7] P. Nicolas, Multifunctional host defense peptides: intracellular-targeting antimicrobial peptides, *FEBS J.* 276 (2009) 6483–6496, <https://doi.org/10.1111/j.1742-4658.2009.07359.x>.
- [8] B.H. Gan, J. Gaynord, S.M. Rowe, T. Deingruber, D.R. Spring, The multifaceted nature of antimicrobial peptides: current synthetic chemistry approaches and future directions, *Chem. Soc. Rev.* 50 (2021) 7820–7880, <https://doi.org/10.1039/d0cs00729c>.
- [9] M. Pirtskhalava, B. Vishnepolsky, M. Grigolava, G. Managadze, Physicochemical features and peculiarities of interaction of amp with the membrane, *Pharmaceuticals* 14 (2021) 1–36, <https://doi.org/10.3390/ph14050471>.
- [10] H. Sato, J.B. Feix, Peptide-membrane interactions and mechanisms of membrane destruction by amphipathic α -helical antimicrobial peptides, *Biochim. Biophys. Acta Biomembr.* 1758 (2006) 1245–1256, <https://doi.org/10.1016/j.bbame.2006.02.021>.
- [11] I. Kabelka, R. Vácha, Advances in molecular understanding of α -helical membrane-active peptides, *Acc. Chem. Res.* 54 (2021) 2196–2204, <https://doi.org/10.1021/acs.accounts.1c00047>.
- [12] L.A. Clifton, M.W.A. Skoda, A.P. Le Brun, F. Ciesielski, I. Kuzmenko, S.A. Holt, J.H. Lakey, Effect of divalent cation removal on the structure of gram-negative bacterial outer membrane models, *Langmuir* 31 (2015) 404–412, <https://doi.org/10.1021/la504407v>.
- [13] M. Smart, A. Rajagopal, W.K. Liu, B.Y. Ha, Opposing effects of cationic antimicrobial peptides and divalent cations on bacterial lipopolysaccharides, *Phys. Rev. E* 96 (2017), <https://doi.org/10.1103/PhysRevE.96.042405>, 0424051–042405–12.
- [14] A.C. Rinaldi, M.L. Mangoni, A. Rufo, C. Luzi, D. Barra, H. Zhao, P.K.J. Kinnunen, A. Bozzi, A. Di Giulio, M. Simmaco, A.R. Fanelli, Temporin L : antimicrobial, haemolytic and cytotoxic activities, and effects on membrane permeabilization in lipid vesicles, *Biochem. J.* 368 (2002) 91–100, <https://doi.org/10.1042/BJ20020806>.
- [15] S. Zhang, M. Ma, Z. Shao, J. Zhang, L. Fu, X. Li, W. Fang, L. Gao, Structure and formation mechanism of antimicrobial peptides Temporin B-and L-induced tubular membrane protrusion, *Int. J. Mol. Sci.* 22 (2021) 1–17, <https://doi.org/10.3390/ijms222011015>.
- [16] H. Zhao, A.C. Rinaldi, A. Di Giulio, M. Simmaco, P.K.J. Kinnunen, Interactions of the antimicrobial peptides temporins with model biomembranes. Comparison of temporins B and L, *Biochemistry* 41 (2002) 4425–4436, <https://doi.org/10.1021/bi011929e>.
- [17] Z. Oren, J.C. Lerman, G.H. Gudmundsson, B. Agerberth, Y. Shai, Structure and organization of the human antimicrobial peptide LL-37 in phospholipid membranes: relevance to the molecular basis for its non-cell-selective activity, *Biochem. J.* 341 (1999) 501–513, <https://doi.org/10.1042/0264-6021:3410501>.
- [18] H. Choi, Z. Yang, J.C. Weisshaar, Oxidative stress induced in *E. coli* by the human antimicrobial peptide LL-37, *PLoS Pathog.* 13 (2017) 1–25, <https://doi.org/10.1371/journal.ppat.1006481>.
- [19] H. Choi, Z. Yang, J.C. Weisshaar, Single-cell, real-time detection of oxidative stress induced in *Escherichia coli* by the antimicrobial peptide CM15, *Proc. Natl. Acad. Sci. U. S. A.* 112 (2015) E303–E310, <https://doi.org/10.1073/pnas.1417703112>.
- [20] D.A. Rowe-Magnus, A.Y. Kao, A.C. Prieto, M. Pu, C. Kao, Cathelicidin Peptides Restrict Bacterial Growth via Membrane Perturbation and Induction of Reactive Oxygen Species, 2019, <https://doi.org/10.1128/mBio>.
- [21] F. Collin, S. Karkare, A. Maxwell, Exploiting bacterial DNA gyrase as a drug target: current state and perspectives, *Appl. Microbiol. Biotechnol.* 92 (2011) 479–497, <https://doi.org/10.1007/s00253-011-3557-z>.
- [22] J.D. Hale, R.E. Hancock, Alternative mechanisms of action of cationic antimicrobial peptides on bacteria, *Expert Rev. Anti Infect. Ther.* 5 (2007) 951–959, <https://doi.org/10.1586/14787210.5.6.951>.
- [23] P. Shah, F.S.H. Hsiao, Y.H. Ho, C.S. Chen, The proteome targets of intracellular targeting antimicrobial peptides, *Proteomics* 16 (2016) 1225–1237, <https://doi.org/10.1002/pmic.201500380>.
- [24] J. Li, P. Fernández-Millán, E. Boix, Synergism between host defense peptides and antibiotics against bacterial infections, *Curr. Top. Med. Chem.* 20 (2020) 1238–1263, <https://doi.org/10.2174/1568026620666200303122626>.
- [25] Q. Feng, Y. Huang, M. Chen, G. Li, Y. Chen, Functional synergy of α -helical antimicrobial peptides and traditional antibiotics against Gram-negative and Gram-positive bacteria in vitro and in vivo, *Eur. J. Clin. Microbiol. Infect. Dis.* 34 (2015) 197–204, <https://doi.org/10.1007/s10096-014-2219-3>.
- [26] L. Duong, S.P. Gross, A. Siryaporn, Developing antimicrobial synergy with AMPs, *Front Med Technol* 3 (2021) 1–8, <https://doi.org/10.3389/fmedt.2021.640981>.
- [27] Y. Huan, Q. Kong, H. Mou, H. Yi, Antimicrobial peptides: classification, design, application and research progress in multiple fields, *Front. Microbiol.* 11 (2020), <https://doi.org/10.3389/fmicb.2020.582779>.
- [28] J. Lu, H. Xu, J. Xia, J. Ma, J. Xu, Y. Li, J. Feng, D- and unnatural amino acid substituted antimicrobial peptides with improved proteolytic resistance and their proteolytic degradation characteristics, *Front. Microbiol.* 11 (2020) 1–17, <https://doi.org/10.3389/fmicb.2020.563030>.
- [29] M.H. Cardoso, R.Q. Orozco, S.B. Rezende, G. Rodrigues, K.G.N. Oshiro, E.S. Cândido, O.L. Franco, Computer-aided design of antimicrobial peptides : are we generating, Effective Drug Candidates ? 10 (2020) 1–15, <https://doi.org/10.3389/fmicb.2019.03097>.
- [30] B. Vishnepolsky, M. Pirtskhalava, Comment on: “Empirical comparison of web-based antimicrobial peptide prediction tools.”, *Bioinformatics* 35 (2019) 2692–2694, <https://doi.org/10.1093/bioinformatics/bty1023/5250704>.
- [31] B. Vishnepolsky, M. Grigolava, G. Managadze, A. Gabrielian, A. Rosenthal, D.E. Hurt, M. Tartakovsky, M. Pirtskhalava, Comparative analysis of machine learning algorithms on the microbial strain-specific AMP prediction, *Briefings Bioinf.* 23 (2022) 1–21, <https://doi.org/10.1093/bib/bbac233>.
- [32] M. Pirtskhalava, A.A. Armstrong, M. Grigolava, M. Chubinidze, E. Alimbarashvili, B. Vishnepolsky, A. Gabrielian, A. Rosenthal, D.E. Hurt, M. Tartakovsky, DBAASP v3: Database of antimicrobial/cytotoxic activity and structure of peptides as a resource for development of new therapeutics, *Nucleic Acids Res.* 49 (2021) D288–D297, <https://doi.org/10.1093/nar/gkaa991>.
- [33] B. Vishnepolsky, G. Zaalishvili, M. Karapetian, T. Nasrashvili, N. Kuljanishvili, A. Gabrielian, A. Rosenthal, D.E. Hurt, M. Tartakovsky, M. Grigolava, M. Pirtskhalava, De novo design and in vitro testing of antimicrobial peptides against gram-negative bacteria, *Pharmaceuticals* 12 (2019), <https://doi.org/10.3390/ph12020082>.
- [34] B. Vishnepolsky, A. Gabrielian, A. Rosenthal, D.E. Hurt, M. Tartakovsky, G. Managadze, M. Grigolava, G.I. Makhatadze, M. Pirtskhalava, Predictive model of linear antimicrobial peptides active against gram-negative bacteria, *J. Chem. Inf. Model.* 58 (2018) 1141–1151, <https://doi.org/10.1021/acs.jcim.8b00118>.
- [35] T.S. Lee, R.A. Krupa, F. Zhang, M. Hajimorad, W.J. Holtz, N. Prasad, S.K. Lee, J.D. Keasling, BglBrick vectors and datasheets: a synthetic biology platform for gene expression, *J. Biol. Eng.* 5 (2011), <https://doi.org/10.1186/1754-1611-5-12>.
- [36] Synergism Testing, Broth microdilution checkerboard and broth macrodilution methods, in: *Clinical Microbiology Procedures Handbook*, ASM Press, 2016, pp. 5.16.1–5.16.23, <https://doi.org/10.1128/9781555818814.ch5.16>.
- [37] S.K. Govers, J. Mortier, A. Adam, A. Aertsen, Protein aggregates encode epigenetic memory of stressful encounters in individual *Escherichia coli* cells, *PLoS Biol.* 16 (2018) 1–40, <https://doi.org/10.1371/JOURNAL.PBIO.2003853>.
- [38] A. Adler, M. Ben-Dalak, I. Chmelitsky, Y. Carmeli, Effect of resistance mechanisms on the inoculum effect of carbenem in *Klebsiella pneumoniae* isolates with borderline carbenem resistance, *Antimicrob. Agents Chemother.* 59 (2015) 5014–5017, <https://doi.org/10.1128/AAC.00533-15>.
- [39] K.S. Thomson, E.S. Moland, Cefepime, piperacillin-tazobactam, and the inoculum effect in tests with extended-spectrum β -lactamase-producing *Enterobacteriaceae*, *Antimicrob. Agents Chemother.* 45 (2001) 3548–3554, <https://doi.org/10.1128/AAC.45.12.3548-3554.2001>.
- [40] A. Rodríguez-Rojas, J. Rolf, Antimicrobial activity of cationic antimicrobial peptides against stationary phase bacteria, *Front. Microbiol.* 13 (2022), <https://doi.org/10.3389/fmicb.2022.1029084>.

- [41] I.C. Mccall, N. Shah, A. Govindan, F. Baquero, B.R. Levin, Antibiotic killing of diversely generated populations of nonreplicating bacteria, *Antimicrob. Agents Chemother.* 63 (2019) 1–13, <https://doi.org/10.1128/AAC.02360-18>.
- [42] U. Rinas, E. García-Fruitós, J.L. Corchero, E. Vázquez, J. Seras-Franzoso, A. Villaverde, Bacterial inclusion bodies: discovering their better half, *Trends Biochem. Sci.* 42 (2017) 726–737, <https://doi.org/10.1016/j.tibs.2017.01.005>.
- [43] E. García-Fruitós, R. Sabate, N.S. De Groot, A. Villaverde, S. Ventura, Biological role of bacterial inclusion bodies: a model for amyloid aggregation, *FEBS J.* 278 (2011) 2419–2427, <https://doi.org/10.1111/j.1742-4658.2011.08165.x>.
- [44] P.M. Oliver, J.A. Crooks, M. Leidl, E.J. Yoon, A. Saghatelian, D.B. Weibel, Localization of anionic phospholipids in *Escherichia coli* cells, *J. Bacteriol.* 196 (2014) 3386–3398, <https://doi.org/10.1128/JB.01877-14>.
- [45] E. Mileykovskaya, W. Dowhan, Visualization of phospholipid domains in *Escherichia coli* by using the cardiolipin-specific fluorescent dye 10-N-nonyl acridine orange, *J. Bacteriol.* 182 (2000) 1172–1175, <https://doi.org/10.1128/JB.182.4.1172-1175.2000>.
- [46] Y. Liu, J.A. Imlay, Cell death from antibiotics without the involvement of reactive oxygen species, *Science* 339 (2013) (1979) 1210–1213, <https://doi.org/10.1126/science.1232751>.
- [47] J. Talapko, T. Meštrović, M. Juzbašić, M. Tomas, S. Erić, L. Horvat Aleksijević, S. Bekić, D. Schwarz, S. Matic, M. Neuberger, I. Škrlec, Antimicrobial peptides—mechanisms of action, antimicrobial effects and clinical applications, *Antibiotics* 11 (2022), <https://doi.org/10.3390/antibiotics11101417>.
- [48] C. Subbalakshmi, N. Sitaram, Mechanism of antimicrobial action of indolicidin, *FEMS Microbiol. Lett.* 160 (1998) 91–96, <https://doi.org/10.1111/j.1574-6968.1998.tb12896.x>.
- [49] C.B. Park, H.S. Kim, S.C. Kim, Mechanism of action of the antimicrobial peptide buforin II: buforin II kills microorganisms by penetrating the cell membrane and inhibiting cellular functions, *Biochem. Biophys. Res. Commun.* 244 (1998) 253–257, <https://doi.org/10.1006/bbrc.1998.8159>.
- [50] J. Yan, K. Wang, W. Dang, R. Chen, J. Xie, B. Zhang, J. Song, R. Wang, Two hits are better than one: membrane-active and DNA binding-related double-action mechanism of NK-18, a novel antimicrobial peptide derived from mammalian NK-lysin, *Antimicrob. Agents Chemother.* 57 (2013) 220–228, <https://doi.org/10.1128/AAC.01619-12>.
- [51] M.R. Loffredo, F. Savini, S. Bobone, B. Casciaro, H. Franzyk, M.L. Mangoni, L. Stella, Inoculum effect of antimicrobial peptides, *Proc. Natl. Acad. Sci. U. S. A.* 118 (2021), <https://doi.org/10.1073/PNAS.2014364118>.
- [52] L. Grassi, M. Di Luca, G. Maisetta, A.C. Rinaldi, S. Esin, A. Trampuz, G. Batoni, Generation of persister cells of *Pseudomonas aeruginosa* and *Staphylococcus aureus* by chemical treatment and evaluation of their susceptibility to membrane-targeting agents, *Front. Microbiol.* 8 (2017) 1–12, <https://doi.org/10.3389/fmicb.2017.01917>.
- [53] E.H. Mood, L. Goltermann, C. Brolin, L.M. Cavaco, A.J. Nejad, N. Yavari, N. Frederiksen, H. Franzyk, P.E. Nielsen, Antibiotic potentiation in multidrug-resistant gram-negative pathogenic bacteria by a synthetic peptidomimetic, *ACS Infect. Dis.* 7 (2021) 2152–2163, <https://doi.org/10.1021/acscinfeddis.1c00147>.
- [54] D.A. Gray, M. Wenzel, Multitarget approaches against multidrug-resistant superbugs, *ACS Infect. Dis.* 6 (2020) 1346–1365, <https://doi.org/10.1021/acscinfeddis.0c00001>.
- [55] D. Zweytick, B. Japelj, E. Mileykovskaya, M. Zorko, W. Dowhan, S.E. Blondelle, S. Riedl, R. Jerala, K. Lohner, N-acylated peptides derived from human lactoferrin perturb organization of cardiolipin and phosphatidylethanolamine in cell membranes and induce defects in *Escherichia coli* cell division, *PLoS One* 9 (2014), <https://doi.org/10.1371/journal.pone.0090228>.
- [56] T.T. Tran, D. Panesso, N.N. Mishra, E. Mileykovskaya, Z. Guan, J.M. Munita, J. Reyes, L. Diaz, G.M. Weinstock, B.E. Murray, Y. Shamoo, W. Dowhan, A.S. Bayer, C.A. Arias, Daptomycin-resistant *Enterococcus faecalis* diverts the antibiotic molecule from the division septum and remodels cell membrane phospholipids, *mBio* 4 (2013) 1–10, <https://doi.org/10.1128/mBio.00281-13>.
- [57] A. Khan, M. Davlieva, D. Panesso, S. Rincon, W.R. Miller, L. Diaz, J. Reyes, M.R. Cruz, O. Pemberton, A.H. Nguyen, S.D. Siegel, P.J. Planet, A. Narechania, M. Latorre, R. Rios, K. V. Singh, H. Ton-That, D.A. Garsin, T.T. Tran, Y. Shamoo, C.A. Arias, Antimicrobial sensing coupled with cell membrane remodeling mediates antibiotic resistance and virulence in *Enterococcus faecalis*, *Proc. Natl. Acad. Sci. USA* 116 (2019) 26925–26932, <https://doi.org/10.1073/pnas.1916037116/-/DCSupplemental>.
- [58] N. Mozaheb, M.P. Mingeot-Leclercq, Membrane vesicle production as a bacterial defense against stress, *Front. Microbiol.* 11 (2020) 1–21, <https://doi.org/10.3389/fmicb.2020.600221>.
- [59] A. De Marco, N. Ferrer-Miralles, E. Garcia-Fruitós, A. Mitraki, S. Peternel, U. Rinas, M.A. Trujillo-Roldán, N.A. Valdez-Cruz, E. Vázquez, A. Villaverde, Bacterial inclusion bodies are industrially exploitable amyloids, *FEMS Microbiol. Rev.* 43 (2019) 53–72, <https://doi.org/10.1093/femsre/fuy038>.
- [60] S. Govindarajan, Y. Elisha, K. Nevo-Dinur, O. Amster-Choder, The general phosphotransferase system proteins localize to sites of strong negative curvature in bacterial cells, *mBio* 4 (2013), <https://doi.org/10.1128/mBio.00443-13>.
- [61] C. Bollen, L. Dewachter, J. Michiels, Protein aggregation as a bacterial strategy to survive antibiotic treatment, *Front. Mol. Biosci.* 8 (2021), <https://doi.org/10.3389/fmolb.2021.669664>.
- [62] S.A. Juliano, L.F. Serafim, S.S. Duay, M. Heredia Chavez, G. Sharma, M. Rooney, F. Comert, S. Pierce, A. Radulescu, M.L. Cotten, M. Mihailescu, E.R. May, A. I. Greenwood, R. Prabhakar, A.M. Angeles-Boza, A potent host defense peptide triggers DNA damage and is active against multidrug-resistant gram-negative pathogens, *ACS Infect. Dis.* 6 (2020) 1250–1263, <https://doi.org/10.1021/acscinfeddis.0c00051>.
- [63] C.W. Gunderson, A.M. Segall, DNA repair, a novel antibacterial target: holliday junction-trapping peptides induce DNA damage and chromosome segregation defects, *Mol. Microbiol.* 59 (2006) 1129–1148, <https://doi.org/10.1111/j.1365-2958.2005.05009.x>.
- [64] Y.H. Hsu, M.W. Chung, T.K. Li, Distribution of gyrase and topoisomerase IV on bacterial nucleoid: implications for nucleoid organization, *Nucleic Acids Res.* 34 (2006) 3128–3138, <https://doi.org/10.1093/nar/gkl392>.
- [65] M. Hartmann, M. Berditsch, J. Hawecker, M.F. Ardakani, D. Gerthsen, A.S. Ulrich, Damage of the bacterial cell envelope by antimicrobial peptides gramicidin S and PGLa as revealed by transmission and scanning electron microscopy, *Antimicrob. Agents Chemother.* 54 (2010) 3132–3142, <https://doi.org/10.1128/AAC.00124-10>.